

ANALYSES OF THE CELLULAR STRUCTURE OF DETONATIONS

J. E. SHEPHERD

Sandia National Laboratories
Albuquerque, NM, USA

I. O. MOEN AND S. B. MURRAY

Defence Research Establishment Suffield
Ralston, Alberta, CANADA

P. A. THIBAUT

Combustion Dynamics, Ltd.
Ralston, Alberta, CANADA

We have investigated the effects of chemical composition and dilution on the regularity of gaseous detonation cellular structure at a fixed critical tube diameter of 52 mm. Three fuel-oxygen mixtures were studied as a function of argon dilution (0% to 80% by volume); the fuels were acetylene, hydrogen and ethane. Smoked foil records were analyzed by digital image processing to obtain a quantitative spectrum of the spatial wavelengths present in the cellular structures. With increasing argon dilution, the number of cells across the tube diameter increases from 4-10 at 0% Ar to 20-30 at 80% Ar at critical transmission conditions for acetylene-oxygen detonations, and the spectra of the cellular structures show a dramatic narrowing in spectral content. A smaller decrease in the dominant spectral wavelength and less increase in regularity with increasing argon dilution are observed for hydrogen-oxygen detonations. Ethane-oxygen detonations have a much more irregular cellular structure and the spectrum is characterized by a broad band of features with the dominant spectral wavelengths independent of argon dilution.

Reaction zone lengths and sensitivity parameters have been computed using the steady-state ZND model of detonation structure. The results of these computations show that these parameters cannot account for the systematic variations in cell regularity and the differences in macroscopic behavior. A partial explanation is offered based on the response of the chemistry to large amplitude variations in shock strength, i.e., degree of overdrive. The amount of overdrive at which the reaction zone becomes endothermic is proposed as a figure of merit for instability and is shown to correlate with present observations.

1. Introduction

The cellular structure of gaseous detonations can be attributed to instabilities in the reacting flow behind the leading shock wave. The spacing observed in the cellular patterns are considerably larger than the induction zone thickness predicted by the steady-state Zel'dovich-von Neumann-Döring (ZND) model of the detonation structure. Numerical simulations of detonations have revealed regular oscillatory patterns when the level of instability is relatively mild.¹⁻³ For highly unstable systems, however, a larger number of instability modes is predicted.³⁻⁵ These modes interact in a nonlinear manner to produce a complex and irregular detonation structure.

A variety of cellular structures have also been

observed experimentally⁵⁻⁷ and the regularity of the cellular structure has been discussed by many authors, including Strehlow⁸ and Libouten and van Tiggelen.⁹ They classified cell structures as excellent, good, poor or irregular depending on the relative strength of the substructure. This classification system is based solely on subjective interpretation of smoked foil records. To date, there have been no attempts to characterize the cellular structure quantitatively.

In spite of the difficulty in interpreting the cellular structure, it has been possible to identify, from smoked foil records, cell sizes for many fuel-oxygen and fuel-air systems.⁹⁻¹³ In fact, the cell width S has been proposed as a fundamental detonation length scale which can be used to characterize the detonability of

gaseous explosives.¹³ A number of correlations and models relating the cell width to a minimum initiation energy and the critical tube diameter for transmission of detonation have been relatively successful.¹⁰⁻¹³ The cell size has also been linked to the chemical reaction kinetics of the mixture through empirical correlations with induction zone length computed for the idealized, one-dimensional ZND model.¹⁴⁻¹⁶

The success of these models and correlations demonstrate the physical significance of the cell width and the relevance of S as a measure of the overall length scale determined by the coupled chemical-gasdynamic processes at the shock front. However, recent experimental results show that the macroscopic behavior of detonations depends not only on the cell size but also on the degree of cell regularity. These findings indicate that parameters and/or length scales in addition to the cell width or induction zone length are required to characterize the macroscopic behavior of detonations. It is therefore important to identify these additional length scales or parameters and to characterize cell irregularity so that fuel-oxidizer systems exhibiting different macroscopic behavior can be classified. As a first step, more detailed quantitative analyses of the smoked foil records could provide means of distinguishing between systems. On the more fundamental level, these differences must be accounted for by the chemical reaction kinetics and gasdynamics of the unstable detonation front.

The present paper reports on the analysis of the cellular structure of detonations in gaseous mixtures exhibiting a wide range of cell regularity. The spectrum of characteristic length scales is determined by applying digital-image-processing techniques to the smoked foil records. These records were obtained in gaseous mixtures having the same critical tube diameter, so that the macroscopic length scale which characterizes transmission from an open tube was fixed. Computations of reaction zone structure using detailed chemical kinetics were performed and correlations between the various length scales are assessed.

2. Experimental Apparatus

The experiments were designed to study differences in detonation cellular structure as a function of fuel type and dilution while holding one detonation length scale (i.e., the critical tube diameter) constant. A set of tests was conducted with three fuel-oxygen mixtures diluted with various amounts (0-80% by vol-

ume) of argon. Fuels used were hydrogen (H_2), acetylene (C_2H_2) and ethane (C_2H_6). The apparatus consisted of a detonation tube 6.8 m long and 52 mm in diameter connected to a large cylindrical vessel 500 mm long and 300 mm in diameter, which simulated an unconfined volume.

Mixtures were prepared by the method of partial pressures. Detonation in the test mixture was initiated by the detonation of a short (0.1-0.25 m) slug of equimolar oxygen-acetylene mixture at the end of the tube. Detonation velocity and pressure were monitored by three pressure transducers positioned along the tube wall. Success or failure of detonation transmission into the larger volume was monitored by a fourth transducer mounted in the end wall of the cylindrical chamber.

For a given mixture composition, tests were conducted at different initial pressures to determine the critical initial pressure for transmission into the large chamber. Subsequent tests at the critical pressure were conducted to record the detonation cellular structure. For this purpose, smoked steel foils (150 mm \times 250 mm \times 0.1 mm in thickness) were inserted into the tube near the exit into the large chamber. Following the test, the smoked foil record was photographed for subsequent image processing.

3. Image Processing of Smoked Foil Records

Smoked foils were analyzed by a digital-image-processing technique. In brief, the technique consists of photographing the foil, digitizing the negative using a scanning microdensitometer, enhancing the resulting digital image, and then computing the two-dimensional Fourier transform by a Fast Fourier Transform method. Peaks in the power spectral density or PSD (defined as the absolute square of the amplitudes of the Fourier components) are used to identify the spatial frequencies present in the image. A detailed exposition of the technique, the theoretical basis for determining cell size from spectra, and results from synthetic and actual data are given by Shepherd and Tieszen.¹⁸

An example smoked foil record is shown in Fig. 1a; this was produced in a test¹⁷ with a mixture of 4.95% C_2H_2 in air at 760 torr initial pressure in an 0.89 m diameter tube. The corresponding PSD computed for this image is shown in Fig. 1b. The information in the two-dimensional PSD is concentrated in two narrow bands of lines, each of which contains independent information about the two separate families of triple-point tracks observed on

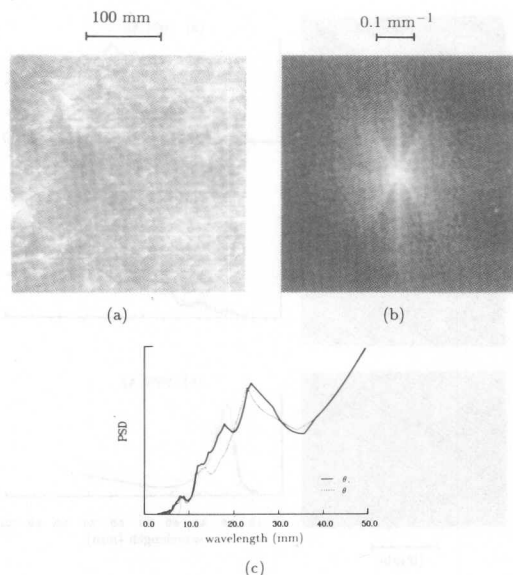


FIG. 1. Example of the image—processing technique applied to a smoked foil detonation record from a mixture of 4.95% C_2H_2 in air inside a 0.89 m diameter tube. (a) Photograph of original record. (b) Power spectral density (PSD) computed from an enhanced digital image of (a). (c) Projections of the PSD onto lines centered on the main power bands.

the smoked foils.‡ These lines of information in the spectral plane are oriented at angles $\alpha \pm$ with respect to the direction of the main detonation propagation. The tracks formed by the triple points themselves are oriented at angles $\Theta \pm = \alpha \pm \mp \pi/2$ to the direction of detonation propagation.

Due to the concentration of information into these narrow bands, the spectra are most simply studied by examining projections of the PSD into lines passing through these bands. Projections of the PSD of Fig. 1b onto these lines are shown in Fig. 1c. The frequency and wavelength scales are appropriate for measurements along the direction transverse to detonation propagation, the usual convention for measuring cell width. While dominant wavelengths can be identified in the plots, a broad spectrum exists. Visual estimates of the cell width range between 10 and 20 mm.

‡By a family of waves or tracks, we mean the total set produced by all waves traveling in the same direction transverse to the main detonation. A circular tube has two families, one rotating clockwise, the other, counterclockwise.

Not all the peaks in the PSD represent fundamental frequencies in the cellular pattern. Harmonics arise simply due to the shape of the intensity variation between the triple-point tracks in the original image. However, the highest amplitude peak is always located at the fundamental frequency. Furthermore, there are numerous types of "irregularity" which have various effects on the resulting PSD.¹⁸ For the purposes of the present paper we note that at least two types of irregularity are observed in the cellular patterns we consider. First, a given transverse wave has a finite lifetime, leading to a finite track length. Second, several different transverse spacings are simultaneously present, corresponding to several natural modes of oscillations.

4. Results and Discussion

4.1 Experimental and Spectral Analyses

The critical tube diameter d_c for successful transmission of a detonation from a round tube into a spherically expanding detonation wave in a surrounding cloud has now been established as a measure of the detonability of a gaseous mixture.¹⁹ For the purposes of the present study, we have kept d_c fixed and focused on the structure of the detonations at criticality for transmission from a 52 mm diameter tube. Criticality is obtained at the value of initial pressure p_c that is bracketed by the GO and NO-GO results for detonation transmission.

Critical initial pressures p_c obtained in the present investigation are shown as a function of argon dilution in Fig. 2. For stoichiometric $C_2H_2-O_2$, p_c increases from 24 torr at 0% Ar to 385 torr at 80% Ar. Tests were also performed with stoichiometric H_2-O_2 and $C_2H_6-O_2$ mixtures at 0, 50, and 75% Ar dilution. Unfortunately, the critical pressure for the 75% Ar cases could not be reached within the safety limits of the apparatus for either of these systems, so that only a lower bound of $p_c > 980$ torr could be obtained.

The mixtures used span a wide range of detonation cell regularity,^{7,17,20} ranging from "excellent" in H_2-O_2 with 50% Ar to "poor" in $C_2H_6-O_2$. Many of the previous investigations were performed in rectangular tubes and the height or width of the tube was only a few cell widths. Under these conditions, there may be a substantial interaction between the acoustic modes of the tube and the natural instability modes of the detonation. By using a round tube and operating under critical conditions, i.e., conditions under which the detonation could successfully transmit to an unconfined cloud,

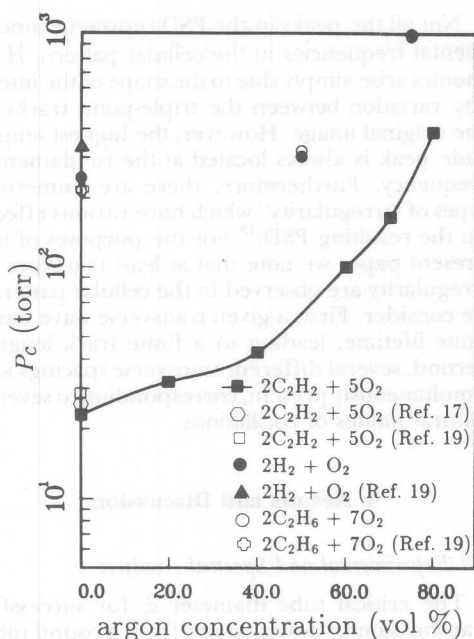


FIG. 2. Critical initial pressure for successful transmission from a 52 mm diameter round tube into an unconfined cloud. Stoichiometric fuel-oxygen mixtures diluted with argon. Data from this paper, Matsui and Lee¹⁹, and Moen *et al.*¹⁷

we have tried to minimize the effects of the tube.

Typical smoked foil records and the one-dimensional projections of the corresponding PSDs are shown in Fig. 3 for stoichiometric $C_2H_2-O_2$ mixtures with 0, 40, and 80% Ar dilution. The most striking feature is that the characteristic length scales are more than a factor-of-two smaller with 80% Ar dilution than with no dilution. The cellular structures at 0 and 40% dilution are very similar both in the level of regularity and in size, with several peaks visible in the PSD. However, there appears to be a shift toward smaller cells at 40% Ar dilution. At 80% Ar dilution, the cellular structure is clearly more regular. This is reflected in the single narrow peak in the PSD.

The trend toward smaller cells and increased regularity with increasing Ar dilution can be seen more clearly in Fig. 4, where the projected PSDs for all dilutions studied are shown together. The wavelengths associated with the peaks in the spectra are plotted vs Ar dilution in Fig. 5. Also shown in this figure are the cell widths measured directly from the smoked foils by visually identifying dominant structures and averaging the track spacing over a number of

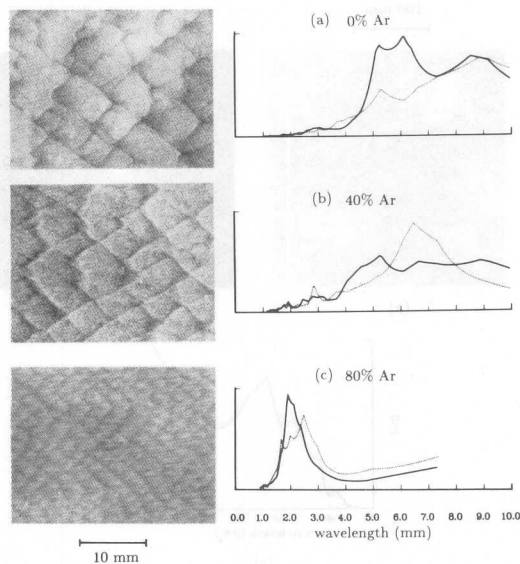


FIG. 3. Smoked foil records and PSD projections at critical conditions for transmission from a 52 mm diameter tube for stoichiometric $C_2H_2-O_2$ mixtures. (a) 0% Ar dilution. (b) 40% Ar dilution. (c) 80% Ar dilution.

clearly defined cells.¹² The cell widths obtained in this manner follow the same trend as the wavelengths obtained by image analysis. However, the richness of the cellular structure's frequency content is completely lost by simply characterizing the structure by an average or dominant cell size.

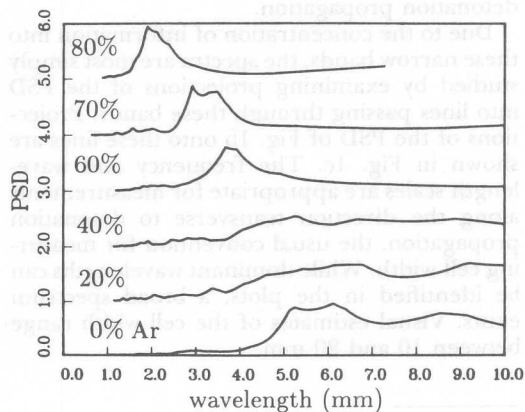


FIG. 4. PSD projections for 0, 20, 40, 60, 70, and 80% Ar dilution of stoichiometric $C_2H_2-O_2$ mixtures at critical conditions for transmission from a 52 mm diameter tube.

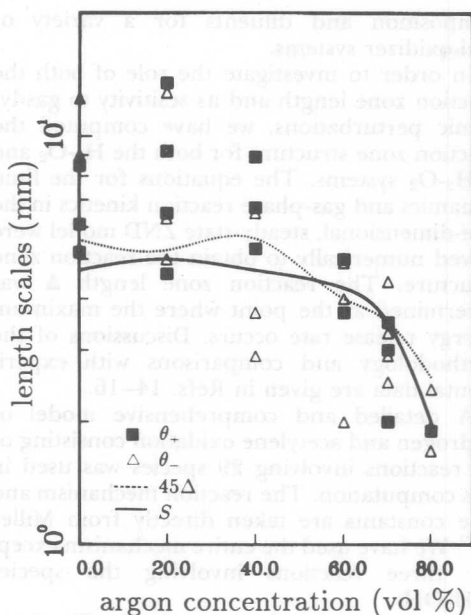


FIG. 5. Cellular pattern length scales from both spectral and visual analysis compared to scaled induction zone lengths (45Δ) for stoichiometric $C_2H_2-O_2$ mixtures as a function of argon concentration. Critical conditions for transmission from a 52 mm diameter tube.

In view of the number of wavelengths that can be identified, it is also difficult to assess the validity of empirical correlation $d_c = 13S$ between the critical tube diameter and the cell width.¹⁰⁻¹³ Depending on the wavelength chosen to represent the cell size, the number of cells across the tube diameter at criticality is 4-10 for 0% Ar and 20-30 for 80% Ar. It must therefore be concluded that a linear relationship between d_c and the wavelengths obtained from smoked foils is not valid for these systems. To a lesser extent this is also true in the H_2-O_2 mixtures. No systematic effect is observed on the spectra of the $C_2H_6-O_2$ systems with Ar dilution.

Smoked foil patterns, together with the corresponding PSDs, are shown in Fig. 6 for two systems: stoichiometric H_2-O_2 diluted with 50% Ar and stoichiometric $C_2H_6-O_2$. According to the classification system of Libouten al,⁷ these mixtures exhibit excellent and poor cell regularity, respectively. Although the cellular pattern observed in $2H_2 + O_2 + 50\% Ar$ is not as regular as that seen by Libouten al⁷ in a rectangular tube, one characteristic dominant wavelength is clearly seen. This is in contrast to

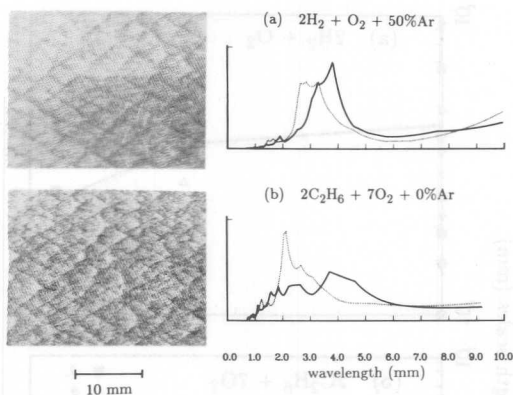


FIG. 6. Smoked foil records and PSD projections for two mixtures at critical conditions for transmission from 52 mm diameter tube. (a) Stoichiometric H_2-O_2 diluted with 50% Ar. (b) Stoichiometric $C_2H_6-O_2$.

the wide spectrum of wavelengths obtained for stoichiometric $C_2H_6-O_2$.

The wavelengths corresponding to the peaks in the PSDs for the H_2-O_2 and $C_2H_6-O_2$ systems are shown in Fig. 7 for different argon dilutions. Also shown are the visually determined cell widths. For the $C_2H_6-O_2$ system there is a wide range of wavelengths, even for high argon dilution, so that it is difficult to associate just one cell size with this system. On the other hand, for H_2-O_2 , the spectrum is fairly narrow and one characteristic wavelength can be defined. For 50% Ar, this wavelength is close to 4 mm, which means that the empirical $d_c = 13S$ correlation is approximately valid in this case. However, cell size measurements at 75% Ar dilution indicate that the cell size at criticality becomes smaller with increased argon dilution, so that the $d_c = 13S$ relationship breaks down in a similar fashion to that observed in the $C_2H_2-O_2$ system.

Some caution should be exercised before attaching too much physical significance to the actual spectrum of wavelengths obtained from the smoked foil records. Firstly, the results are obtained by the analysis of one record for each mixture. Although this analysis typically includes a large number of "cells," it can not be considered a comprehensive statistical analysis. Secondly, the spectrum of wavelengths is influenced by the boundary conditions. Detonations in other configurations, geometries, and away from criticality could have a different spectrum of wavelengths. However, the image-processing results do show that different chemical systems exhibit different cellular structure for a fixed

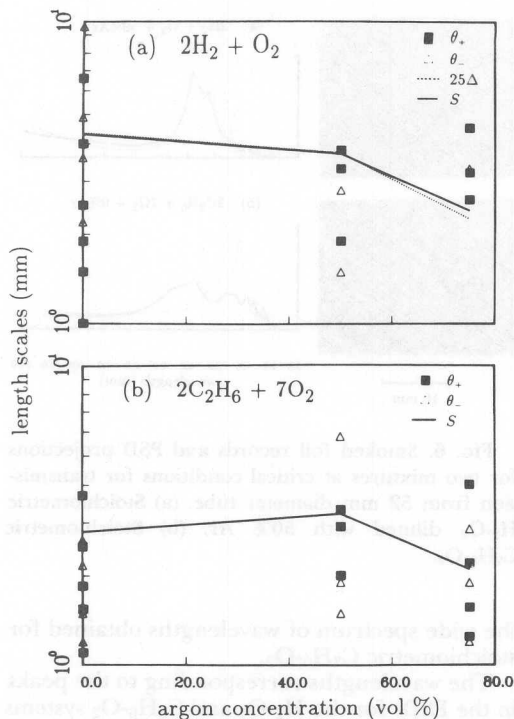


Fig. 7. Cellular pattern length scales from both spectral and visual analysis compared to scaled induction zone lengths (25Δ) for mixtures of stoichiometric (a) $\text{H}_2\text{-O}_2$ and (b) $\text{C}_2\text{H}_6\text{-O}_2$ as a function of argon concentration. Critical conditions for transmission from a 52 mm diameter tube.

geometry and a constant value of sensitivity, i.e., a fixed critical tube diameter. Furthermore, the rich spectrum of cellular patterns typically found on a smoked foil record is clearly revealed by the image analysis. It is also clear from this analysis that one unique "cell size" cannot, in general, be defined based solely on the patterns observed on smoked foil records.

4.2 Detailed Chemical Kinetics Computations

The cellular structure of detonations is a reflection of the stability of the wave as well as the fundamental chemical reaction kinetics and gasdynamic processes within the detonation front. From previous investigations, it has been found that the induction zone length is typically one to two orders-of-magnitude smaller than the "cell size." In spite of this disparity, linear correlations between cell width and reaction zone length have been relatively successful in predicting the variation of cell width with

composition and diluents for a variety of fuel-oxidizer systems.

In order to investigate the role of both the reaction zone length and its sensitivity to gasdynamic perturbations, we have computed the reaction zone structure for both the $\text{H}_2\text{-O}_2$ and $\text{C}_2\text{H}_6\text{-O}_2$ systems. The equations for the fluid dynamics and gas-phase reaction kinetics in the one-dimensional, steady-state ZND model were solved numerically to obtain the reaction zone structure. The reaction zone length Δ was determined as the point where the maximum energy release rate occurs. Discussions of the methodology and comparisons with experimental data are given in Refs. 14–16.

A detailed and comprehensive model of hydrogen and acetylene oxidation consisting of 97 reactions involving 29 species was used in this computation. The reaction mechanism and rate constants are taken directly from Miller *et al.*²¹ We have used the entire mechanism except for three reactions involving the species $\text{C}_4\text{H}_2\text{OH}$.

As an example of our results, in Fig. 5 we compare a constant multiple of the reaction zone length (45Δ) with the length scales determined for $\text{C}_2\text{H}_6\text{-O}_2$ with various argon dilutions. The correct prediction of the general trend indicates that some link does exist between the reaction zone length and these length scales. For $\text{H}_2\text{-O}_2$ mixtures, the comparison with 25Δ is shown in Fig. 7; the behavior is similar to that seen in the acetylene system.

Qualitative criteria have also been proposed to account for irregular cellular structures. These criteria are derived from theories of detonation stability.²² For wavelengths much longer than the reaction zone thickness, the level of instability generally increases with the global activation energy E_A for the mixture. This is in qualitative agreement with the observation that the irregularity of the structure increases with the value of E_A/RT , where T is the postshock temperature and R is the gas constant.²³ This parameter is related to the sensitivity of the induction time τ to small changes in the Mach number M about the CJ value M_{CJ} ,¹⁷ which has been used to characterize the stability of detonations to small perturbations.^{24,25}

The parameter $-\frac{\delta\tau}{\tau} / \frac{\delta M}{M}$ was computed numerically using a constant-volume approximation to the reaction zone and $\sim 1\%$ variations in M to obtain $\delta\tau$. The values of this parameter are given in Table I. Based on stability theory, we expect that less stable systems with more irregular cellular structures will be associated with larger values of this parameter. From the values given in Table I, it

TABLE I

Experimentally measured critical pressures and calculated chemical kinetic parameters for stoichiometric $C_2H_2-O_2-Ar$, H_2-O_2-Ar , and $C_2H_6-O_2-Ar$ mixtures at critical conditions for transmission through a 52 mm diameter tube. Also included are the parameters for a C_2H_2 -air detonation.

Fuel	% Ar	p_c (torr)	Δ (mm)	$-(\delta\tau/\tau)/(\delta M/M)$	$f^* = (M^*/M_{CJ})^2$
C_2H_2	0	23	0.124	5.00	2.39
C_2H_2	20	32	0.117	5.03	2.35
C_2H_2	40	43	0.125	5.12	2.21
C_2H_2	60	100	0.089	5.24	2.09
C_2H_2	75	165	0.078	5.34	2.06
C_2H_2	80	385	0.057	5.45	2.06
H_2	0	245	0.174	7.53	3.07
H_2	50	302	0.149	6.64	2.34
H_2	75	990 ^a	0.090	6.63	2.22
C_2H_6	0	215	—	—	3.21
C_2H_6	50	320	—	—	2.52
C_2H_6	75	975 ^a	—	—	2.31
$C_2H_2^b$	0	760	0.070	5.10	3.90

^a subcritical conditions

^b 4.95% in air, 0.89 m dia tube

appears that this parameter cannot account for the levels of cell irregularity observed in the present tests. For example, in the $C_2H_2-O_2$ system this parameter is only weakly dependent on the amount of argon dilution, and the trend is opposite to that predicted by the simple stability theory. For H_2-O_2 mixtures, the stability parameter does decrease with increasing argon dilution, opposite to the trend observed in $C_2H_2-O_2$. The values of the parameter range from 7.5 to 6.6, much larger than the value of 5.1 computed for the C_2H_2 -air example that has a very irregular structure.

The failure of correlations and criteria based on ZND computations for CJ detonations is not too surprising. It is well-established that the shock velocity within a detonation cell oscillates between 0.8 and 1.6 times the CJ value. Although CJ conditions characterize the *average* state, most of the chemical reactions do not occur at these *average* condition.²⁶ In fact, most reactions probably take place at temperatures that are higher than the postshock (von Neumann) value behind a CJ wave.

In order to determine the influence of these variations in shock strength on the chemical processes, we have computed the reaction zone structure for a range of 0.5 to 1.5 times M_{CJ} . The constant-volume approximation was used to compute the induction time for both the stoichiometric $C_2H_2-O_2$ and H_2-O_2 mixtures with Ar dilution. For both fuels, the effective activation energies change abruptly for $M \geq$

$1.2M_{CJ}$. This is due to the increased importance of high-activation-energy dissociation processes at elevated postshock temperatures. For C_2H_2 , the net result is an increase in the effective activation energy; for H_2 , the effective activation energy decreases. This distinctly non-Arrhenius behavior will affect the stability of the reaction zone and should be included in any realistic treatment of detonation stability.

As the overdrive is increased, the net energy release rate will eventually vanish due to a balance between endothermic dissociation processes and exothermic recombination of radical species. This balance will limit the amplitude of the shock oscillations. Simple thermochemical computations can be used to determine the amount of overdrive required to obtain the onset of endothermic reaction and we propose that it may be used as a figure of merit to characterize the degree of instability and the resulting irregularity of detonation cellular structures.

The critical overdrive factors ($f^* = (M^*/M_{CJ})^2$) for which the reaction initially becomes endothermic are given in Table I. In order of largest-to-smallest f^* values, the mixtures are ranked as: C_2H_2 -air, $C_2H_6-O_2$, H_2-O_2 , and $C_2H_2-O_2$. This is also the order of increasing regularity, with ethane being a possible exception. The increasing regularity of H_2-O_2 and $C_2H_2-O_2$ detonations with increasing argon dilution is accompanied by decreasing values of f^* . Computations with N_2 dilution instead of Ar

show that the value of f^* increases with dilution; this trend agrees with experimental observations on cell irregularity in those systems.

The parameter f^* cannot be the single controlling factor since the present ethane results and the dramatic effect of inhibitors on cellular structure cannot be explained in this fashion. Without a more complete understanding of the instability mechanisms and the coupling between gasdynamics and chemical reaction within the cellular detonation front, this relationship cannot be put on a firm footing. However, the association of regular structure with systems which become endothermic at low amounts of overdrive could account for the observed difference in macroscopic transmission and propagation behavior of detonations in regular and irregular systems.¹⁷

Transmission of detonations from a tube with a central obstacle plate, for example, involves reinitiation due to the implosion of the diffracted shock waves.²⁷ The temperature and pressure in the central implosion region are much higher than those behind a shock wave with CJ velocity. We therefore expect that endothermic behavior will set in at a much earlier time for systems that are associated with regular cell structure than those with irregular structure, so that reinitiation will be inhibited in regular systems relative to more irregular systems. This trend is exactly what is observed experimentally.¹⁷

Similar arguments can also be used to account for the failure of detonations in small tubes. The lowest mode of propagation in a round tube is single-head spin, whereby a detonation propagates in a helical fashion around the periphery of the tube with a velocity of about 1.6 times the CJ velocity.²⁸ Failure would therefore be expected to occur much more readily in systems that are prone to endothermic behavior. This is, again, exactly what is observed.

By carrying these arguments one step further, it is also possible to account for the decrease in cell wavelengths observed at a fixed critical tube size for increasing amounts of argon dilution. Reinitiation at criticality occurs near the apex of the cone formed by the expansion from the diffraction aperture, and the reinitiated wave sweeps through the pre-shocked region of the cone.²⁵ Since the resulting temperatures are much higher than those behind a CJ wave in an unshocked region, endothermic behavior could inhibit the propagation of the sweeping reinitiation wave. This implies that the successful transmission of detonation would require a more chemically sensitive mixture, that is, one with smaller characteristic length scales.

5. Conclusions

Image-processing analyses of smoked foil records obtained in detonations of gas mixtures exhibiting a wide range of cell regularity demonstrate a rich spectrum of wavelengths in the features of the cellular structure. In general, the more irregular the structure, the richer the wavelength spectra. A unique dominant wavelength can only be identified in those mixtures with an exceptionally regular structure.

It has also been shown that it is necessary to characterize not only the reaction zone length but also the response of the reaction zone to large amplitude perturbations in shock strength. Reaction zone computations using detailed chemical reaction kinetics demonstrate that the mixture composition can play a crucial role in determining this response. Although the connection between cell regularity and the large-amplitude response of the reaction zone is somewhat tenuous at the present time, it is certainly plausible. A number of recent observations on macroscopic detonation response can be explained by such a connection.

Acknowledgments

We would like to thank Marc Lauzon, Stephan Lesage, Chris Brosinsky and Keith Gerrard of DRES for their valuable assistance in performing the laboratory tests from which the experimental data were extracted. We also thank the Photo Group at DRES for their assistance in photographing the smoked foil records and the Photometrics Division at Sandia for digitizing these records. Portions of this work were performed at Sandia National Laboratories which is operated for the U.S. Department of Energy under contract number DE-AC04-76DP00789.

REFERENCES

1. TAKI, A. AND FUJIWARA, T.: *AIAA J.* 16, 73 (1978).
2. KAILASANATH, K., ORAN, E.S., BORIS, J.P. AND YOUNG, T. R.: *Combust. Flame* 61, 199 (1985).
3. ABOUSIEF, G.F. AND TOONG, T.Y.: *Combust. Flame* 45, 67 (1982).
4. ERPENBECK, J.J.: *Phys. Fluids* 9, 684 (1964).
5. MOEN, I.O., FUNK, S.W., WARD, S.A., RUDE, G.M., AND THIBAUT, P.A.: *AIAA Prog. Astro. and Aero.* 94, 55 (1984).
6. STREHLOW, R.A.: *Astronautica Acta* 14, 539 (1969).
7. LIBOUTEN, J-C. AND VAN TIGGELEN, P.J.: *Proceedings of the First Specialist Meeting (Internat-*

- tional) on Combustion, p. 437, Bordeaux, France, July, 1981.
8. STREHLOW, R.A.: *Combust. Flame* 18, 59 (1968).
 9. STREHLOW, R.A. AND ENGEL, C.D.: *AIAA J.* 7, 492 (1969).
 10. BULL, D.C., ELLSWORTH, J.E., AND SCHUFF, P.F.: *Combust. Flame* 45, 7 (1982).
 11. KNYSTAUTAS, R., LEE, J.H., AND GUIRAO, C.: *Combust. Flame* 48, 63, (1982).
 12. MOEN, I. O., MURRAY, S. B., BJERKETVEDT, D., RINNAN, A., KNYSTAUTAS, R. AND LEE, J. H.: Nineteenth Symposium (International) on Combustion, p. 635, The Combustion Institute, 1982.
 13. LEE, J. H.: *Ann. Rev. of Fluid Mech.* 16, 311, 1984.
 14. WESTBROOK, C. K. AND URTIEW, P. A.: Nineteenth Symposium (International) on Combustion, p. 615, The Combustion Institute, 1982.
 15. SHEPHERD, J. E.: *Detonation Modeling and Reaction Kinetics in Hydrogen-Air-Diluent Mixtures*. Presentation at the Tenth International Colloquium on Dynamics of Explosions and Reactive Systems, Berkeley, CA, USA, August, 1985.
 16. SHEPHERD, J. E., SULMISTRAS, A., SABER, A. J. AND MOEN, I. O.: *Chemical Kinetics and Cellular Structure of Detonations in Hydrogen Sulphide and Air*. Presentation at the Tenth International Colloquium on Dynamics of Explosions and Reactive Systems, Berkeley, CA, USA, August, 1985.
 17. MOEN, I. O., SULMISTRAS, A., THOMAS, G. O., BJERKETVEDT, D. AND THIBAUT, P. A.: *The Influence of Cellular Regularity on the Behavior of Gaseous Detonations*. Presentation at the Tenth International Colloquium on Dynamics of Explosions and Reactive Systems, Berkeley, CA, August, 1985.
 18. SHEPHERD, J. E. AND TIESZEN, S. R.: *Detonation Cellular Structure and Image Processing*. Sandia National Laboratories Report SAND86-0033, 1986.
 19. MATSUI, H. AND LEE, J. H.: Seventeenth Symposium (International) on Combustion, p. 1269, The Combustion Institute, 1978.
 20. VANDERMEIREN, M. AND VAN TIGGELEN, P. S.: *AIAA Prog. in Astro. Aero.* 94, 104, (1984).
 21. MILLER, J. A., MITCHELL, R. E., SMOOKE, M. D., AND KEE, R. J.: Nineteenth Symposium (International) on Combustion, p. 181, The Combustion Institute, 1982.
 22. FICKETT, W. AND DAVIS, W. C.: *Detonation*, University of California Press, 1979.
 23. UL'YANITSKII, V. YU.: *Fizika Goreniya Vzryva* 17, 127 (1981).
 24. SHCHELKIN, K. I.: *Zh. Eksp. Teor. Fiz.* 36, 600 (1959).
 25. EDWARDS, D. H., THOMAS, G. O. AND WILLIAMS, T. L.: *J. Fluid Mech.* 95, 79 (1979).
 26. LIBOUTEN, J.-C., DORMAL, M. AND VAN TIGGELEN, P.J.: *AIAA Prog. Astro. Aero.* 75, 358 (1981).
 27. THILBAULT, P. A., BJERKETVEDT, D., SULMISTRAS, A., THOMAS, G. O., JENSSEN, A. AND MOEN, I.O.: *The Role of Energy Distribution on the Transmission of Gaseous Detonations into the Unconfined*. Presentation at the Tenth International Colloquium on Dynamics of Explosions and Reactive Systems, Berkeley, CA, August, 1985.
 28. VOITSEKHOVSKII, B. V., MITROFANOV, V. V., AND TOPCHIAN, M. E.: *Fiz. Goreniya Vzryva* 5, 385 (1969).

COMMENTS

M. Stock, Battelle Institute, W. Germany. The amount of irregularity you measure should be influenced by the boundary conditions as well as by the mixture properties. Would you comment on this influence?

Author's Reply. Previous studies have shown a substantial effect due to the confining geometry whenever the detonation cell width is comparable to the smallest dimension of the apparatus. This interaction is accompanied by an increase in regularity due to resonance between the intrinsic detonation instability and the acoustic modes of the tube. Our experiments were carried out under critical tube conditions and the tube diameter was 13 to 30 times larger than the cell widths. Interactions between the tube acoustic modes and the detonation structure are expected to be much weaker under these conditions.

Since our technique for quantifying cellular structure has only recently been developed, no systematic investigation of the effect of varying the ratio of cell width to tube size (λ/d) has been made.

●

C. O. Leiber, B.I.C.T., W. Germany. Please, what is the basic mechanism of soot deposition? For example, is the triple point mechanism confirmed or assumed? I am presently performing calculations on a multi-spherical source model, and I get cells in pressure, impedance, particle velocities, streamlines . . . , and I would like to know which results are found in your investigations?

Author's Reply. The soot is not deposited but merely rearranged by the detonation wave and associated

instabilities. No information about the fundamental mechanism of track formation was obtained in this investigation. The production of the sooted-foil tracks was shown to unambiguously correspond to

the triple point trajectories by Lee et al. [Lee, J. H., Soloukhin, R. I. and Oppenheim, A. K.: *Astronautica Acta* 14, 565-584 (1969)].

18. Mataré H and Lee J. H. *Spacecraft Symposia*, vol. 1, McGraw-Hill, New York, 1969, p. 1503.

19. Mataré H and Lee J. H. *Spacecraft Symposia*, vol. 2, McGraw-Hill, New York, 1970, p. 1503.

20. Mataré H and Lee J. H. *Spacecraft Symposia*, vol. 3, McGraw-Hill, New York, 1971, p. 1503.

21. Mataré H and Lee J. H. *Spacecraft Symposia*, vol. 4, McGraw-Hill, New York, 1972, p. 1503.

22. Mataré H and Lee J. H. *Spacecraft Symposia*, vol. 5, McGraw-Hill, New York, 1973, p. 1503.

23. Mataré H and Lee J. H. *Spacecraft Symposia*, vol. 6, McGraw-Hill, New York, 1974, p. 1503.

24. Mataré H and Lee J. H. *Spacecraft Symposia*, vol. 7, McGraw-Hill, New York, 1975, p. 1503.

25. Mataré H and Lee J. H. *Spacecraft Symposia*, vol. 8, McGraw-Hill, New York, 1976, p. 1503.

26. Mataré H and Lee J. H. *Spacecraft Symposia*, vol. 9, McGraw-Hill, New York, 1977, p. 1503.

27. Mataré H and Lee J. H. *Spacecraft Symposia*, vol. 10, McGraw-Hill, New York, 1978, p. 1503.

28. Mataré H and Lee J. H. *Spacecraft Symposia*, vol. 11, McGraw-Hill, New York, 1979, p. 1503.

29. Mataré H and Lee J. H. *Spacecraft Symposia*, vol. 12, McGraw-Hill, New York, 1980, p. 1503.

30. Mataré H and Lee J. H. *Spacecraft Symposia*, vol. 13, McGraw-Hill, New York, 1981, p. 1503.

31. Mataré H and Lee J. H. *Spacecraft Symposia*, vol. 14, McGraw-Hill, New York, 1982, p. 1503.

32. Mataré H and Lee J. H. *Spacecraft Symposia*, vol. 15, McGraw-Hill, New York, 1983, p. 1503.

33. Mataré H and Lee J. H. *Spacecraft Symposia*, vol. 16, McGraw-Hill, New York, 1984, p. 1503.

34. Mataré H and Lee J. H. *Spacecraft Symposia*, vol. 17, McGraw-Hill, New York, 1985, p. 1503.

35. Mataré H and Lee J. H. *Spacecraft Symposia*, vol. 18, McGraw-Hill, New York, 1986, p. 1503.

36. Mataré H and Lee J. H. *Spacecraft Symposia*, vol. 19, McGraw-Hill, New York, 1987, p. 1503.

37. Mataré H and Lee J. H. *Spacecraft Symposia*, vol. 20, McGraw-Hill, New York, 1988, p. 1503.

38. Mataré H and Lee J. H. *Spacecraft Symposia*, vol. 21, McGraw-Hill, New York, 1989, p. 1503.

39. Mataré H and Lee J. H. *Spacecraft Symposia*, vol. 22, McGraw-Hill, New York, 1990, p. 1503.

40. Mataré H and Lee J. H. *Spacecraft Symposia*, vol. 23, McGraw-Hill, New York, 1991, p. 1503.

41. Mataré H and Lee J. H. *Spacecraft Symposia*, vol. 24, McGraw-Hill, New York, 1992, p. 1503.

42. Mataré H and Lee J. H. *Spacecraft Symposia*, vol. 25, McGraw-Hill, New York, 1993, p. 1503.

43. Mataré H and Lee J. H. *Spacecraft Symposia*, vol. 26, McGraw-Hill, New York, 1994, p. 1503.

44. Mataré H and Lee J. H. *Spacecraft Symposia*, vol. 27, McGraw-Hill, New York, 1995, p. 1503.

45. Mataré H and Lee J. H. *Spacecraft Symposia*, vol. 28, McGraw-Hill, New York, 1996, p. 1503.

46. Mataré H and Lee J. H. *Spacecraft Symposia*, vol. 29, McGraw-Hill, New York, 1997, p. 1503.

47. Mataré H and Lee J. H. *Spacecraft Symposia*, vol. 30, McGraw-Hill, New York, 1998, p. 1503.

48. Mataré H and Lee J. H. *Spacecraft Symposia*, vol. 31, McGraw-Hill, New York, 1999, p. 1503.

49. Mataré H and Lee J. H. *Spacecraft Symposia*, vol. 32, McGraw-Hill, New York, 2000, p. 1503.

50. Mataré H and Lee J. H. *Spacecraft Symposia*, vol. 33, McGraw-Hill, New York, 2001, p. 1503.

51. Mataré H and Lee J. H. *Spacecraft Symposia*, vol. 34, McGraw-Hill, New York, 2002, p. 1503.

52. Mataré H and Lee J. H. *Spacecraft Symposia*, vol. 35, McGraw-Hill, New York, 2003, p. 1503.

53. Mataré H and Lee J. H. *Spacecraft Symposia*, vol. 36, McGraw-Hill, New York, 2004, p. 1503.

54. Mataré H and Lee J. H. *Spacecraft Symposia*, vol. 37, McGraw-Hill, New York, 2005, p. 1503.

55. Mataré H and Lee J. H. *Spacecraft Symposia*, vol. 38, McGraw-Hill, New York, 2006, p. 1503.

56. Mataré H and Lee J. H. *Spacecraft Symposia*, vol. 39, McGraw-Hill, New York, 2007, p. 1503.

57. Mataré H and Lee J. H. *Spacecraft Symposia*, vol. 40, McGraw-Hill, New York, 2008, p. 1503.

58. Mataré H and Lee J. H. *Spacecraft Symposia*, vol. 41, McGraw-Hill, New York, 2009, p. 1503.

59. Mataré H and Lee J. H. *Spacecraft Symposia*, vol. 42, McGraw-Hill, New York, 2010, p. 1503.

60. Mataré H and Lee J. H. *Spacecraft Symposia*, vol. 43, McGraw-Hill, New York, 2011, p. 1503.

61. Mataré H and Lee J. H. *Spacecraft Symposia*, vol. 44, McGraw-Hill, New York, 2012, p. 1503.

62. Mataré H and Lee J. H. *Spacecraft Symposia*, vol. 45, McGraw-Hill, New York, 2013, p. 1503.

63. Mataré H and Lee J. H. *Spacecraft Symposia*, vol. 46, McGraw-Hill, New York, 2014, p. 1503.

64. Mataré H and Lee J. H. *Spacecraft Symposia*, vol. 47, McGraw-Hill, New York, 2015, p. 1503.

65. Mataré H and Lee J. H. *Spacecraft Symposia*, vol. 48, McGraw-Hill, New York, 2016, p. 1503.

66. Mataré H and Lee J. H. *Spacecraft Symposia*, vol. 49, McGraw-Hill, New York, 2017, p. 1503.

67. Mataré H and Lee J. H. *Spacecraft Symposia*, vol. 50, McGraw-Hill, New York, 2018, p. 1503.

68. Mataré H and Lee J. H. *Spacecraft Symposia*, vol. 51, McGraw-Hill, New York, 2019, p. 1503.

69. Mataré H and Lee J. H. *Spacecraft Symposia*, vol. 52, McGraw-Hill, New York, 2020, p. 1503.

70. Mataré H and Lee J. H. *Spacecraft Symposia*, vol. 53, McGraw-Hill, New York, 2021, p. 1503.

71. Mataré H and Lee J. H. *Spacecraft Symposia*, vol. 54, McGraw-Hill, New York, 2022, p. 1503.

72. Mataré H and Lee J. H. *Spacecraft Symposia*, vol. 55, McGraw-Hill, New York, 2023, p. 1503.

73. Mataré H and Lee J. H. *Spacecraft Symposia*, vol. 56, McGraw-Hill, New York, 2024, p. 1503.

74. Mataré H and Lee J. H. *Spacecraft Symposia*, vol. 57, McGraw-Hill, New York, 2025, p. 1503.

COMMENTS

At least three points W. Conway, The mission of research for nuclear should be informed by the positive conditions as well as by the nuclear properties. Would you comment on the following:

Authors' reply: Previous studies have shown a substantial effect due to the current geometry whenever the discharge cell with a comparable to the smallest dimension of the apparatus. The mission is accompanied by an increase in regarding the resonance between the nuclear discharge unit and the second member of the tube. Our experiments were carried out under critical conditions and the discharge was 15 to 20 times larger than the cell width. Resonance between the tube current member and the discharge system is expected to be much weaker under these conditions.

Authors' reply: The ion is not captured but merely scattered by the formation wave and associated

Since our objective for developing cellular systems has only recently been extended to maintain synchronization of the effect of varying the rate of cell width in order to vary the flow rate.

E. O. Johnson, B.A.C., W. Conway, Please with a few last conditions of our experiment. For example, is the triple point mechanism captured or resonant? I am presently performing experiments on a multi-physics source model and I get cells in pressure independent points of cellular conditions. ... and I would like to know which results are found in your investigations.